nature physics

ARTICLES

PUBLISHED ONLINE: 17 MAY 2009 | DOI: 10.1038/NPHYS1276

Individual topological tunnelling events of a quantum field probed through their macroscopic consequences

Mitrabhanu Sahu[1]*, Myung-Ho Bae[1], Andrey Rogachev[1,2], David Pekker[1,3], Tzu-Chieh Wei[1,4], Nayana Shah[1], Paul M. Goldbart[1] and Alexey Bezryadin[1]

Phase slips are topological fluctuations that carry the superconducting order-parameter field between distinct current-carrying states. Owing to these phase slips, superconducting nanowires acquire electrical resistance. In such wires, it is well known that at higher temperatures phase slips occur through the process of thermal barrier-crossing by the order-parameter field. At low temperatures, the general expectation is that phase slips should proceed through quantum tunnelling events, which are known as quantum phase slips. However, resistive measurements have produced evidence both for and against the occurrence of quantum phase slips. Here, we report evidence for the observation of individual quantum phase-slip events in homogeneous ultranarrow wires at high bias currents. We accomplish this through measurements of the distribution of switching currents for which the width exhibits a rather counter-intuitive, monotonic increase with decreasing temperature. Importantly, measurements show that in nanowires with larger critical currents, quantum fluctuations dominate thermal fluctuations up to higher temperatures.

Quantum phenomena involving macroscopic degrees of freedom and occurring in systems far larger than individual atoms are one of the most exciting fields of modern physics. Initiated by Leggett more than 25 years ago, the field of macroscopic quantum tunnelling[1–5] (MQT) has seen widespread development, important realizations being furnished, such as, by MQT of the phase in Josephson junctions[6–9], and MQT of the magnetization in magnetic nanoparticles[10]. More recently, the breakthrough recognition of the potential advantages of quantum-based computational methods has initiated the search for viable implementations of qubits[11,12], several of which are rooted in MQT in superconducting systems. In particular, it has recently been proposed that superconducting nanowires (SCNWs) could provide a valuable setting for realizing qubits[13]. In this case, the essential behaviour needed of SCNWs is that they undergo quantum phase slip[14] (QPS), that is, topological quantum fluctuations of the superconducting order-parameter field through which tunnelling occurs between current-carrying states, replacing the thermally activated Little phase slips[15], occurring at higher temperatures. It has also been proposed that QPS in nanowires could enable one to build a current standard, and thus could have a useful role in aspects of metrology[16]. In addition, QPSs are believed to provide the pivotal processes underpinning the superconductor–insulator transition observed in nanowires[17–22]. Observations of QPS have been reported previously on wires with high normal resistance ($R_N > R_Q$, where $R_Q = h/4e^2 \approx 6,450\ \Omega$) through low-bias resistance (R) versus temperature (T) measurements[14,23–25]. Yet, low-bias measurements on short wires with normal resistance $R_N < R_Q$ have been unable to reveal QPS (refs 26–28). In addition, it has been suggested that some results ascribed to QPS could in fact have originated in inhomogeneity of the nanowires[29]. Thus, no consensus exists about the conditions under which QPSs occur, and qualitatively new evidence for QPS remains highly desirable.

Here, we present measurements of the distribution of stochastic switching currents—the high-bias currents at which the resistance exhibits a sharp jump from a very small value to a much larger one, close to R_N—in $Mo_{79}Ge_{21}$ nanowires. We observe a monotonic increase in the width of the distribution as the temperature is decreased. We analyse these findings in light of a new theoretical model[30], which incorporates Joule heating[31] caused by stochastically occurring phase slips. The switching rates yielded by the model are quantitatively consistent with the data, over the entire range of temperatures at which measurements were carried out (0.3–2.2 K), provided that both QPS and thermally activated phase slip[15,32,33] (TAPS) processes are included. In contrast, if only TAPSs are included, the model fails to give qualitative agreement with our observed switching-rate behaviour below 1.2 K. Thus, we conclude that in our SCNWs, the phase of the superconducting order-parameter field slips predominantly through thermal activation at high temperatures; however, at temperatures below 1.2 K, it is quantum tunnelling that dominates the phase-slip rate. It is especially noteworthy that at even lower temperatures (below 0.7 K) both our data and the model suggest that each individual phase slip causes switching of the wire to the resistive state. In other words, there is one-to-one correspondence between unobservable phase slips and easily observable switching events. Thus, in this regime, one has the capability of exploring the physics of single quantum phase-slip events. Furthermore, we observe strong effects of QPS

[1]Department of Physics, University of Illinois at Urbana Champaign, 1110 West Green Street, Urbana, Illinois 61801, USA, [2]Department of Physics, University of Utah, 115 S 1400 E, Salt Lake City, Utah 84112, USA, [3]Department of Physics, Harvard University, 17 Oxford Street, Cambridge, Massachusetts 02138, USA, [4]Institute for Quantum Computing and Department of Physics and Astronomy, University of Waterloo, 200 University Ave. W., Waterloo, Ontario N2L 3G1, Canada. *e-mail: sahu@illinois.edu.

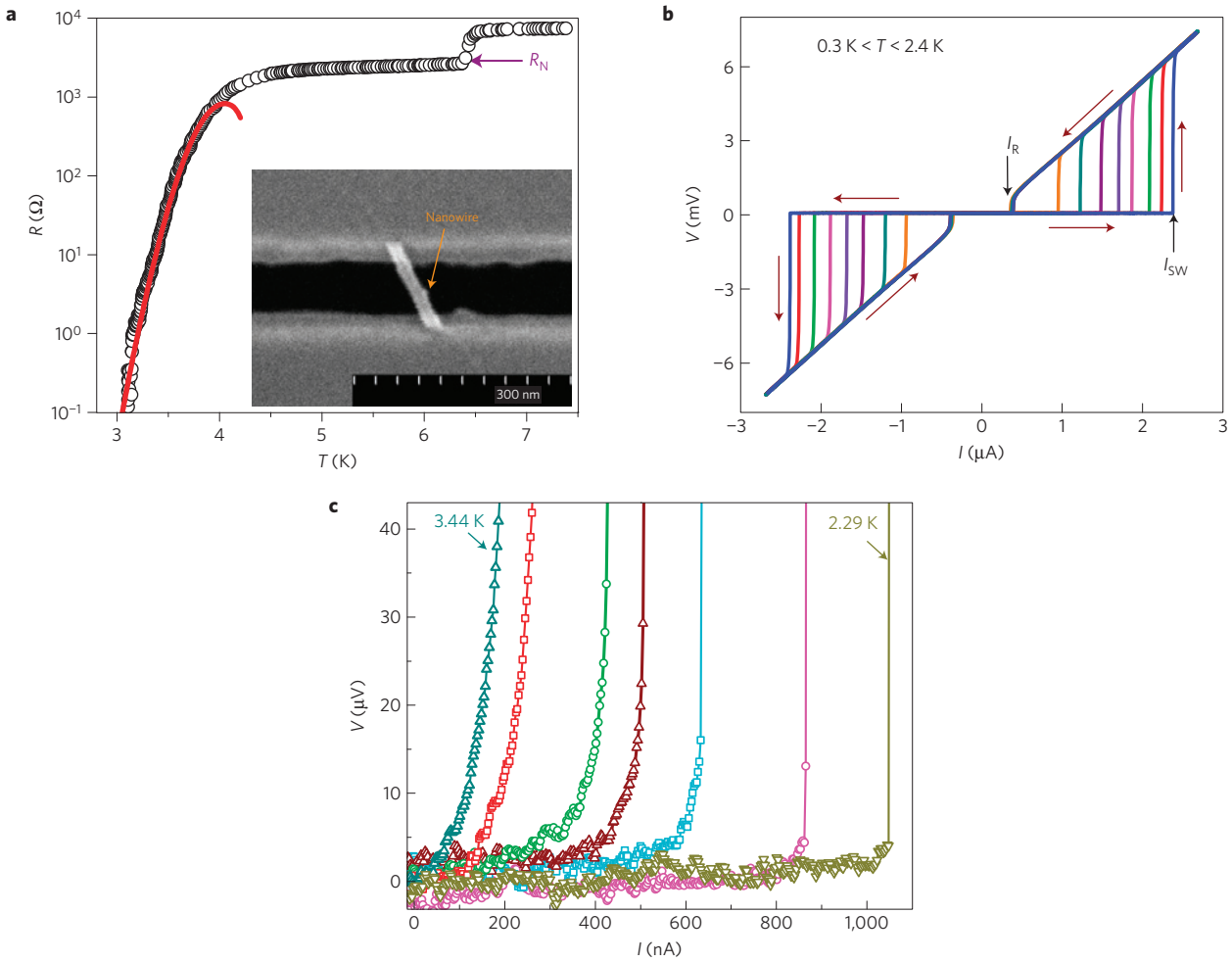

Figure 1 | Basic sample characterization at high and low temperatures. a, Zero-bias resistance versus temperature measurement (sample S1). The circles are the data and the solid line is the fit to the LAMH model. The normal-state resistance of the wire, R_N, is indicated by the arrow, which is measured immediately below the film transition. Our set-up allows measurements down to 0.1 Ω, which is reached already at $T = 3.0$ K. Inset: Scanning electron microscope image of nanowire sample S1. **b**, Voltage versus current dependence at various temperatures from 2.3 to 0.3 K for wire S1. The switching current I_{SW} and retrapping current I_R are indicated for the data taken at 0.3 K. The temperatures are $T = 0.3$ (the highest I_{SW}), 0.6, 0.9, 1.2, 1.5, 1.8, 2.1, 2.4 K. **c**, Residual voltage tails observed at high-bias currents, just before the switching. The temperatures are $T = 3.44$, 3.33, 3.11, 3.0, 2.85, 2.49, 2.29 K. These voltage tails become smaller as the temperature is decreased and become immeasurably low for $T < \sim 2.5$ K.

at high bias currents, even in wires with $R_N < R_Q$. Another crucial fact is that the observed quantum behaviour is more pronounced in wires with larger critical currents. This fact enables us to rule out the possibility that the observed behaviour is caused by noise or wire inhomogeneity.

Low-bias measurements

The linear low-bias resistance for the wire S1 is shown in Fig. 1a. The resistance measured just below the temperature at which the thin-film leads become superconducting is taken as the normal-state resistance R_N of the wire. We find that the superconducting transition of the wire is well described by the phenomenological model of TAPSs in a quasi-one-dimensional superconductor developed by Langer–Ambegaokar[32] and McCumber–Halperin[33] (LAMH). To fit the R versus T data, we have used the expression: $R(T) = [R_{LAMH}^{-1}(T) + R_N^{-1}]^{-1}$ (ref. 23). The resistance due to TAPS is given by, $R_{LAMH}(T) = (\pi\hbar^2\Omega(T)/2e^2k_BT)\exp(-(\Delta F(T)/k_BT))$, where $\Delta F(T)$ is the free-energy barrier for a phase slip in the zero-bias regime and $\Omega(T)$ is the attempt frequency (see Supplementary Information text)[34]. The fitting parameters used are the critical temperature $T_C = 4.34$ K and the zero-temperature Ginzburg–Landau coherence length $\xi(0) = 8.2$ nm. As the temperature is decreased, the resistance becomes exponentially suppressed, and eventually falls below our experimental resolution. In contrast with the works of Giordano[14] and Lau *et al.*[23], we do not find tails in the R versus T data, which would indicate QPS, probably because R_N is significantly lower for our wires. As an attempt to find the QPS regime, we have opted to make measurements at high bias currents, near the critical current, at low temperatures, that is, in the regime in which the QPS rate should exceed the TAPS rate[31].

High-bias switching-current measurements

A representative set of voltage–current characteristics $V(I)$, measured at various temperatures, is shown in Fig. 1b. These data show that, as the bias current is swept from low to high, the system exhibits an abrupt transition from a zero or extremely low-voltage state (that is, a superconducting state) to a high-voltage state in which the resistance is close to R_N (that is, a normal state). We call the current at which the switching occurs, the switching current I_{SW}. Similarly, as the bias current is swept from high to low, the wire reverts to being superconducting, doing so at a retrapping current I_R. We indicate these currents in Fig. 1b for data taken at 0.3 K. As can be seen from Fig. 1b, our nanowires are strongly hysteretic: there is a regime of currents within which

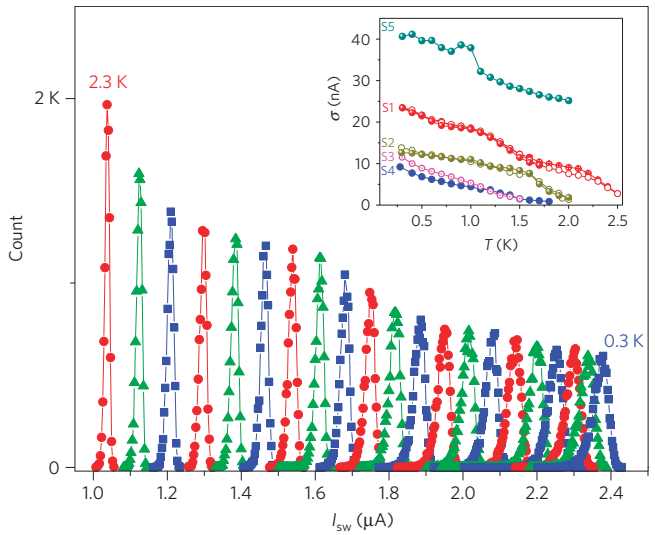

Figure 2 | Switching-current distributions at different temperatures. Switching-current distributions $P(I_{SW})$ for temperatures between 0.3 K (right-most) and 2.3 K (left-most) with $\Delta T = 0.1$ K for sample S1. For each distribution, 10,000 switching events were recorded and the bin size of the histograms was 3 nA. Inset: Standard deviation $\sigma (= \sqrt{(\sum_{i=1}^{n} (I_{SW,i} - \bar{I}_{SW})^2)/(n-1)})$ of $P(I_{SW})$ versus T for five different nanowires including sample S1. For samples S1 and S2, the measurements were repeated a few times to verify the reproducibility of the temperature dependence of σ. For all wires, the width of the distributions increases as the temperature is decreased.

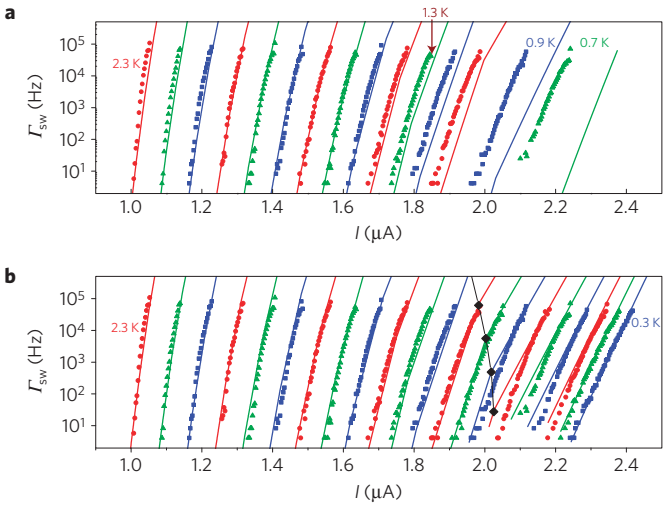

Figure 3 | Measured switching rates from the superconducting state and predictions of the stochastic overheating model. a, Switching rates from the superconducting state to the resistive state for bath temperatures between 2.3 K (left-most) and 0.7 K (right-most) (here not all of the measured curves are shown, for clarity). The data are shown for all temperatures between 2.3 K and 1.1 K with $\Delta T = 0.1$ K and for $T = 0.9$ K and $T = 0.7$ K (sample S1). The symbols are experimental data and the lines (with corresponding colour) are fits to the overheating model that incorporates stochastic TAPS-only (see text). The fits agree well with the data down to 1.3 K, indicated by an arrow. **b**, Fits to the same data (all temperatures are shown here) with the stochastic overheating model that now incorporates both the TAPS and QPS rates to calculate the switching rates. The boundary for the single-phase-slip switch regime is indicated by the black diamond symbols at four temperatures (connected by line segments). For the measured range of switching rates, any of the (I, Γ_{SW}) to the right of this boundary (that is, for higher bias currents) is in the single-slip regime.

the wire is bistable (that is, two voltage states, one superconductive and one normal, are locally stable), and one of the two states is realized depending on the history of the current sweep. We also find I_{SW} is stochastic whereas I_R is not, within our experimental resolution (~0.5 nA).

The stochasticity corresponds to the observation that even when the temperature and current-sweep protocol are kept fixed, I_{SW} varies from run to run, resulting in a distribution of switching currents $P(I_{SW})$, as was first studied for Josephson junctions by Fulton and Dunkleberger[35]. Such distributions, obtained at various temperatures, reflect the underlying, stochastically fluctuating, collective dynamics of the condensate, and therefore provide a powerful tool for shedding light on the nature of the quasi-one-dimensional superconductivity. Indeed, one would expect the distribution width to scale with the thermal noise, and hence to decrease, as the temperature is reduced[35]; and to saturate at low temperature where thermal fluctuations are frozen out and only quantum fluctuations are left[7].

To obtain $P(I_{SW})$ at a particular temperature, we applied a triangular-wave current (sweep rate 125.5 μA s^{-1} and amplitude 2.75 μA), and recorded I_{SW} (see Fig. 1b) for each of 10,000 cycles. We repeated this procedure at 21 equally spaced temperatures between 0.3 and 2.3 K, thus arriving at the normalized distributions shown in Fig. 2. We observe the broadening of the switching-current distribution as the temperature is lowered, which is the exact opposite of the Fulton–Dunkleberger result[35]. This is our main observation, which is analysed in detail below. This trend is confirmed by the analysis of the standard deviations σ of the distributions for samples S1, S2, S3, S4 and S5; see Fig. 2 (inset). We would like to mention that the slight bump in the σ data for the wire S5, observed at 0.9–1 K, is due to a total of three anomalous points, out of 20,000 points, which are most probably caused by factors extrinsic to our measurement set-up and thus should be neglected (see Supplementary Information for a detailed discussion). The (R_N, L) for these five samples, S1, S2, S3, S4 and S5, are (2,662 Ω, 110 nm), (4,100 Ω, 195 nm), (1,430 Ω, 104 nm), (3,900 Ω, 200 nm) and (1,450 Ω, 120 nm), respectively. Following the Fulton–Dunkleberger result, we have transformed our $P(I_{SW})$ data into information on the rates $\Gamma_{SW}(I, T)$ at which switching would occur at a fixed current and temperature[35]. The switching rates resulting from the data in Fig. 2 are shown in Fig. 3.

To understand the origin of the peculiar dependence of the switching-current distribution on temperature, we review mechanisms that could be responsible for the switching from the superconducting to the resistive state, and their implications for the switching-current distributions. It is evident from the observed variability of the switching current that, to be viable, a candidate for the switching mechanism must be stochastic in nature. This suggests that the switching events are triggered by intrinsic fluctuations in the wire. In what follows, we shall focus on mechanisms driven by phase-slip fluctuations.

Current-switching driven by phase-slip fluctuations

The simplest mechanism to consider is the one in which a single phase slip necessarily causes switching to the resistive state, as in an under-damped Josephson junction[35]. In fact, in our wires, at temperatures $T > \sim 1$ K, the rate of TAPS as indicated by both low-bias R–T and high-bias V–I measurements, is always expected to be much larger than the observed switching rate, even at very low currents. Therefore, at these temperatures, a current-carrying wire undergoes many TAPSs before the switch takes place, as directly confirmed by the non-zero voltage regime observed before the switching[27,36]; as shown in Fig. 1c (also see Supplementary Fig. S1 and Supplementary Information text). For $T > 2.7$ K, we

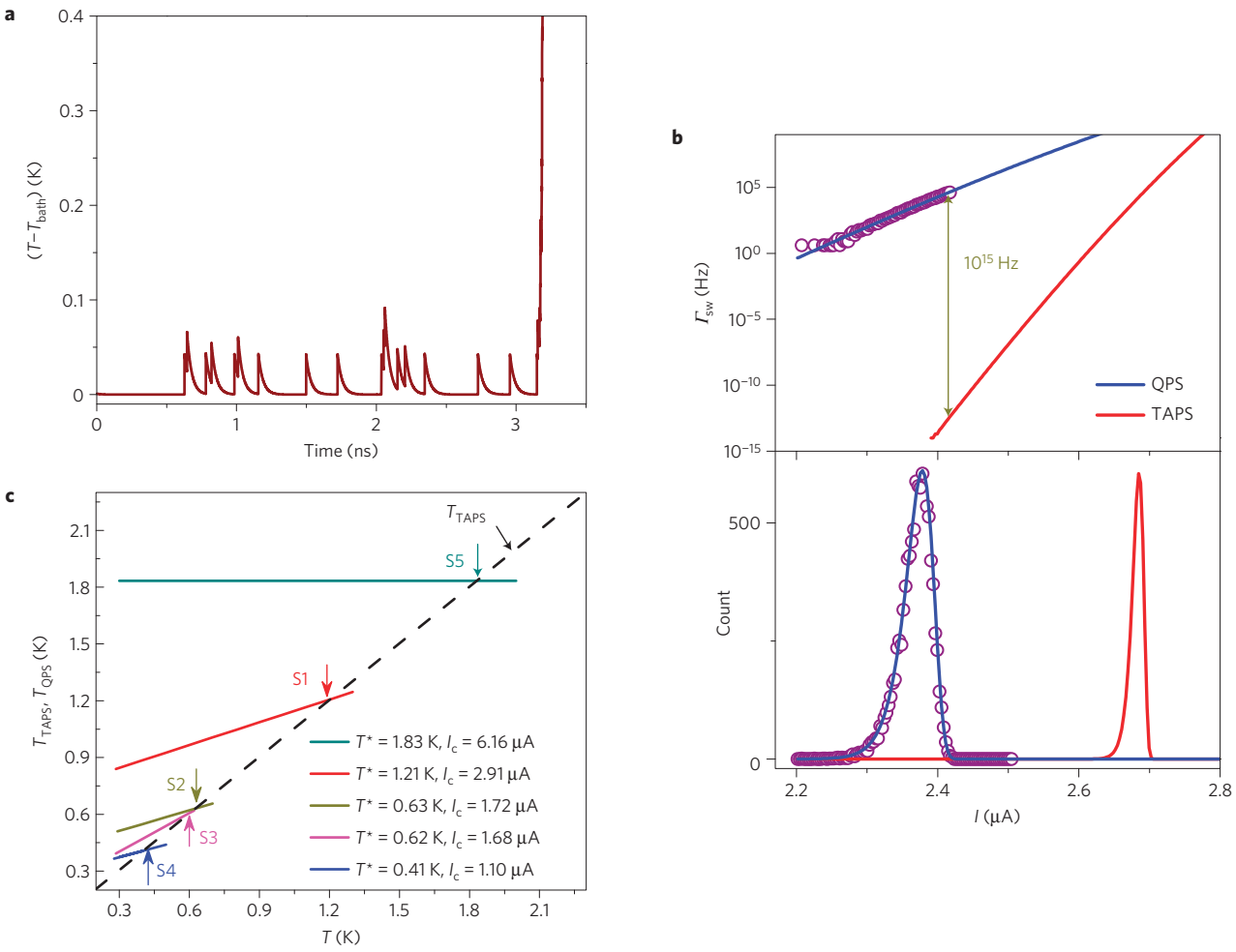

Figure 4 | Stochastic phase slips, switching rates and the quantum behaviour at low temperatures. a, Simulated 'temperature bumps' in the nanowire due to a sequence of phase-slips events. The bath temperature is assumed to be $T_b = 2.4$ K, $T_C = 3.87$ K and bias current $I = 1.0$ μA. As the temperature of the wire section becomes higher than T_C, it becomes normal. **b**, Top panel: Switching rates at $T = 0.3$ K for sample S1 (open circles). The blue curve is the fit to the data, based on the Giordano-type QPS model. The red curve is expected for the TAPS rate. The arrow indicates the difference between the expected TAPS rate and the data. This difference is very large, namely 10^{15} Hz. Bottom panel: The corresponding switching-current distribution at 0.3 K (open circles) and the predictions due to the QPS rate (blue) and the TAPS rate (red). **c**, The best-fit effective temperature for fluctuations at different bath temperatures for five different samples (S1–S5). For all TAPS rate calculations, the effective temperature is chosen as the bath temperature (shown by the black dashed line). For the QPS rates, the effective temperature T_{QPS}, used in the corresponding QPS fits, similar to the blue-line fits of **b**, is shown by the solid lines. For each sample, below the crossover temperature T^* (indicated by arrows), QPS dominates the TAPS. We find that the T^* decreases with decreasing critical depairing current of the nanowires, which is the strongest proof of QPS. The trend indicates that the observed behaviour of T_{QPS} below T^* is not due to extraneous noise in the set-up or granularity of wires, but, indeed, is due to QPS.

can measure these residual voltage tails occurring at a current lower than the switching current. As the temperature is reduced, these voltage tails, indicating a non-zero phase-slip rate, become smaller, and below ~2.5 K the voltage falls below the experimental resolution of our set-up (~2 μV). The quantitative analysis of the switching process[30] leads us to the conclusion that the switching is activated by multiple phase slips at $T > \sim 1$ K and by single phase slips at $T < \sim 1$ K.

We now focus on switching mechanisms that incorporate multiple phase slips. The observed high-voltage state is inconsistent with the presence of a phase-slip centre, because there is almost no offset current. We therefore hypothesize that the dynamics is always over-damped, and propose a runaway overheating model in the spirit of ref. 31. Our model has two ingredients: (1) stochastic phase slips that heat the wire by a quantum of energy $I\,h/2e$, and occur at random times and locations in the wire, but with a rate that depends on the local temperature of the wire and (2) the heat produced by the phase slips is conducted along the wire, and is carried away by the leads. In effect, right after a phase slip has occurred, the temperature of the wire rises, and therefore the phase-slip rate is enhanced. The higher phase-slip rate persists until the wire cools down. If another phase slip happens to occur before the wire has cooled down, the temperature would rise further. Moreover, if, after several consecutive phase slips, the temperature in the wire becomes high enough for the phase-slip rate to exceed the cooling rate, a subsequent cascade of phase slips carries the wire into the high-voltage state, which is the normal state. Thus, the switching is stochastic in nature. The rate of this switching is directly determined by the likelihood of having an initial burst of phase slips that starts a cascade. This phenomenology is captured in Fig. 4a, which shows the temperature at the centre of a wire (above the bath temperature) as a function of time. Phase slips correspond to sudden jumps in temperature, whereas cooling corresponds to the gradual decrease of temperature. A burst of phase slips that results in a cascade can be seen near time $t = 3$ ns.

In the overheating model just discussed, the width of the switching-current distribution is controlled by the competition between the number of phase slips in the cascade-triggering burst and the rate of phase slips. If the number of phase slips to make such a burst tends to unity, the switching rate approaches the phase-slip rate. In the opposite regime, in which a large number of phase slips are required to form the burst, the switching rate is much lower than the phase-slip rate. At higher temperatures, many phase slips are needed in the initial burst, and thus switching tends to occur only when I_{SW} is in a very narrow range close to I_C, thus making the distribution narrow (see Supplementary Fig. S2). As the temperature decreases, the heat capacity and heat conductivity both decrease, making phase slips more effective at heating the wire. Thus, the typical number of phase slips in the cascade-triggering burst decreases with temperature, as our model shows[30]. At the same time, the rate of TAPS also decreases with temperature. In practice, with decreasing temperature, the broadening effect of the burst length on $P_{SW}(I)$ overwhelms the narrowing effect of the decreasing TAPS rate, and this provides a possible explanation for the unanticipated broadening of the I_{SW} distributions.

We first tried to fit all of the switching-rate data in Fig. 3 using the overheating model but with a phase-slip rate Γ that follows from allowing only thermally activated (and not quantum) processes, that is, Γ_{TAPS}. At temperature T and bias-current I, Γ_{TAPS} is given by,

$$\Gamma_{TAPS}(T,I)=\frac{\Omega_{TAPS}(T)}{2\pi}\exp\left(-\frac{\Delta F(T,I)}{k_BT}\right)$$

where $\Omega_{TAPS}(T)$ is the attempt frequency, $\Delta F(T,I)=\Delta F(T)(1-(I/I_C(T)))^{5/4}$ is the free-energy barrier at bias-current I (refs 31, 32), $I_C(T)$ is the fluctuation-free depairing current and $\Delta F(T)=\sqrt{6}(\hbar I_C(T)/2e)$ is the free-energy barrier at zero bias-current[37] (see Supplementary Information text). These fits agree well with the data over the temperature range 2.4–1.3 K (Fig. 3a). Within this range, we can attribute the decrease in the width of the distribution to the mechanism described in the previous paragraph: the competition between (1) the number of phase slips in the initial burst required to start a cascade and (2) the rate of phase slips. However, below 1.2 K, it is evident from Fig. 3a that the switching rates predicted by TAPS are considerably smaller than the switching rates obtained experimentally.

Switching in the single-phase-slip regime

As the temperature is reduced and fluctuations become smaller, the switching happens at higher values of the bias-current I. Thus, each phase slip releases more heat into the wire ($I\,h/2e$). In addition, as the bias-current I is increased, the value of the temperature increase required to reach the normal state becomes smaller. Therefore, according to the overheating model, one ultimately expects to have a low T regime in which a single phase-slip event releases enough heat to induce a switching event[30]. We call this the single-slip regime. We expect that for $T<\sim 0.7$ K, the wire S1 should be operating in this single-slip regime, as indicated in Fig. 3b (the black curve). We find, however, in the regime $0.3\,\mathrm{K}<\mathrm{T}<1.2\,\mathrm{K}$ our data cannot be fitted well if the phase-slip rate is taken to be $\Gamma_{TAPS,}$ but can be fitted well if the total phase-slip rate (Γ_{TOTAL}) is taken to be the sum of the TAPS rate (Γ_{TAPS}) and the QPS rate (Γ_{QPS}) (that is, $\Gamma_{TOTAL}=\Gamma_{TAPS}+\Gamma_{QPS}$). As at 0.3 K we are already in the single-slip regime, the switching rate should be equal to the phase-slip rate. As shown in Fig. 4b, at 0.3 K, the measured switching rate can be fitted by the Giordano-type QPS rate[14], given by the same expression as the TAPS rate but with the wire temperature T replaced by an effective 'quantum' temperature $T_{QPS}(T)$, that is, $\Gamma_{QPS}(T,I)=(\Omega_{QPS}(T)/2\pi)\exp(-\Delta F(T,I)/k_BT_{QPS})$ (see Supplementary Information text)[14,23]. For $T=0.3$ K, the switching rate predicted by TAPS is roughly 10^{15} times smaller than the measured switching rate (Fig. 4b, top panel). Using different expressions for the attempt frequency (such as those derived for Josephson junctions) can only increase the disagreement between the TAPS model and the data (see Supplementary Information text and Supplementary Fig. S3). On the other hand, fitting the measured switching rate with the Giordano-type QPS rate for several values of the temperature, we find a very good agreement. The corresponding effective quantum temperature $T_{QPS}(T)$ is considerably higher than the bath temperature T, which is a strong indication of QPS. We also observe that to fit data, it is necessary to assume a weak linear dependence of the $T_{QPS}(T)$ on the bath temperature T (Fig. 4c). For sample S1, T_{QPS} is found to be $T_{QPS}(T)=0.726+0.40\times T$ (in kelvins). The non-zero intercept indicates the persistence of the high-bias-current-induced QPS down to zero temperature. It is found that below a crossover temperature T^*, the QPS rate dominates over the TAPS rate and the fluctuations in the nanowire are mostly quantum in nature. This T^* for wire S1 is 1.2 K and is denoted by the red arrow in Fig. 4c (see Supplementary Information text). To verify the consistency of our model at all measured temperatures, we replaced the TAPS rate by the total phase-slip rate Γ_{TOTAL} to obtain the switching rates over the full range of temperatures (that is, 0.3–2.3 K). We find that the predicted switching rates agree reasonably well with the data, as shown in Fig. 3b for all temperatures.

Furthermore, we verified the evidence of QPS in four more nanowire samples (S2–S5). The function $T_{QPS}(T)$ (which we define to be linear in all cases) for these nanowires is shown in Fig. 4c. As with the first sample, this linear dependence is chosen to give the best possible fits to the measured switching rates, as shown in Fig. 4b. In addition, the corresponding crossover temperatures T^* for all samples are indicated by the arrows. We find that the T^* is consistently reduced with the reduction of the critical depairing current $I_C(0)$, as shown in Fig. 4c (see Supplementary Information for details). This observed trend is analogous to the case of Josephson junctions in ref. 7. To understand this observation, we recall that T^* is proportional to the plasma frequency of the device, which, in turn, is proportional to the critical current. On the other hand, if the observed increase in the fluctuation strength and the fact that $T_{QPS}>T$ were due to some uncontrolled external noise in the set-up, the thicker wires, having larger critical currents, would have shown a reduction in the T^*, which is opposite to what we observe. These observations also enable us to rule out the possibility that some hidden granularity causes the QPS-like effects. Indeed, what we find is that wires of lower critical currents, which obviously have more chance to have weak links, show a less pronounced quantum behaviour and a lower T^* value (Fig. 4c). Thus, the possibility of weak links producing the QPS-like effects reported here is ruled out. In conclusion, the result of Fig. 4c provides qualitatively new and strong evidence for the existence of QPS in thin superconducting wires.

Methods

Our nanowires were fabricated using molecular templating[17]. Amorphous $Mo_{79}Ge_{21}$ alloy was sputtered onto fluorinated single-wall carbon nanotubes that were suspended across 100–200-nm-wide trenches[38]. The wires appear quite homogeneous in scanning electron microscope images, such as in the inset of Fig. 1a. The nanowire is seamlessly connected to thin-film $Mo_{79}Ge_{21}$ leads at each of its ends. All of our measurements were carried out in a ^{3}He cryostat with the base temperature ~285 mK. All signal lines were equipped with room-temperature (7 dB cutoff frequency of 3 MHz, Spectrum Control) and copper powder and silver-paste microwave filters kept at the base temperature (see Supplementary Information). For the signal lines with all of the filtering, the measured attenuation is larger than 100 dB for frequencies higher than 1 GHz (see Supplementary Fig. S6). The voltage signals were amplified using battery-powered, low-noise preamplifiers (SR 560). The samples were measured with a four-probe configuration as described in ref. 17.

Received 19 September 2008; accepted 15 April 2009; published online 17 May 2009

References

1. Leggett, A. J. Prospects in ultralow temperature physics. *J. Phys. Colloq.* **39**, 1264–1269 (1978).
2. Leggett, A. J. Macroscopic quantum systems and the quantum theory of measurement. *Prog. Theor. Phys. Suppl.* **69**, 80–100 (1980).
3. Caldeira, A. O. & Leggett, A. J. Influence of dissipation on quantum tunneling in macroscopic systems. *Phys. Rev. Lett.* **46**, 211–214 (1981).
4. Leggett, A. J. *Lesson of Quantum Theory. N. Bohr Centenary Symposium* 35–57 (North-Holland, 1986).
5. Leggett, A. J. *et al.* Dynamics of the dissipative two-state system. *Rev. Mod. Phys.* **59**, 1–85 (1987).
6. Voss, R. F. & Webb, R. A. Macroscopic quantum tunneling in 1-μm Nb Josephson junctions. *Phys. Rev. Lett.* **47**, 265–268 (1981).
7. Martinis, J. M., Devoret, M. H. & Clarke, J. Experimental tests for the quantum behavior of a macroscopic degree of freedom: The phase difference across a Josephson junction. *Phys. Rev. B* **35**, 4682–4698 (1987).
8. Inomata, K. *et al.* Macroscopic quantum tunneling in a *d*-wave high-T_C $Bi_2Sr_2CaCu_2O_{8+\delta}$ superconductor. *Phys. Rev. Lett.* **95**, 107005 (2005).
9. Wallraff, A. *et al.* Quantum dynamics of a single vortex. *Nature* **425**, 155–158 (2003).
10. Wernsdorfer, W. *et al.* Macroscopic quantum tunneling of magnetization of single ferrimagnetic nanoparticles of barium ferrite. *Phys. Rev. Lett.* **79**, 4014–4017 (1997).
11. Shor, P. *Proc. 35th Annual Symposium on Foundations of Computer Science* 124–134 (1994).
12. Shor, P. Polynomial-time algorithms for prime factorization and discrete logarithms on a quantum computer. *SIAM J. Computing* **26**, 1484–1509 (1997).
13. Mooij, J. E. & Harmans, C. J. P. M. Phase-slip flux qubits. *New J. Phys.* **7**, 219 (2005).
14. Giordano, N. Evidence for macroscopic quantum tunneling in one-dimensional superconductors. *Phys. Rev. Lett.* **61**, 2137–2140 (1988).
15. Little, W. A. Decay of persistent currents in small superconductors. *Phys. Rev.* **156**, 396–403 (1967).
16. Mooij, J. E. & Nazarov, Y. V. Superconducting nanowires as quantum phase-slip junctions. *Nature Phys.* **2**, 169–172 (2006).
17. Bezryadin, A., Lau, C. N. & Tinkham, M. Quantum suppression of superconductivity in ultrathin nanowires. *Nature* **404**, 971–974 (2000).
18. Bollinger, A. T., Dinsmore, R. C. III, Rogachev, A. & Bezryadin, A. Determination of the superconductor–insulator phase diagram for one-dimensional wires. *Phys. Rev. Lett.* **101**, 227003 (2008).
19. Zaikin, A. D., Golubev, D. S., vanOtterlo, A. & Zimanyi, G. T. Quantum phase slips and transport in ultrathin superconducting wires. *Phys. Rev. Lett.* **78**, 1552–1555 (1997).
20. Meidan, D., Oreg, Y. & Refael, G. Sharp superconductor–insulator transition in short wires. *Phys. Rev. Lett.* **98**, 187001 (2007).
21. Khlebnikov, S. & Pryadko, L. P. Quantum phase slips in the presence of finite-range disorder. *Phys. Rev. Lett.* **95**, 107007 (2005).
22. Khlebnikov, S. Quantum phase slips in a confined geometry. *Phys. Rev. B* **77**, 014505 (2008).
23. Lau, C. N., Markovic, N., Bockrath, M., Bezryadin, A. & Tinkham, M. Quantum phase slips in superconducting nanowires. *Phys. Rev. Lett.* **87**, 217003 (2001).
24. Altomare, F., Chang, A. M., Melloch, M. R., Hong, Y. & Tu, C. W. Evidence for macroscopic quantum tunneling of phase slips in long one-dimensional superconducting Al wires. *Phys. Rev. Lett.* **97** 17001 (2006).
25. Zgirski, M., Riikonen, K.-P., Touboltsev, V. & Arutyunov, K. Yu. Quantum fluctuations in ultranarrow superconducting aluminum nanowires. *Phys. Rev. B* **77**, 054508 (2008).
26. Bollinger, A. T., Rogachev, A. & Bezryadin, A. Dichotomy in short superconducting nanowires: Thermal phase slippage versus coulomb blockade. *Europhys. Lett.* **76**, 505–511 (2006).
27. Rogachev, A. & Bezryadin, A. Superconducting properties of polycrystalline Nb nanowires templated by carbon nanotubes. *Appl. Phys. Lett.* **83**, 512–514 (2003).
28. Rogachev, A., Bollinger, A. T. & Bezryadin, A. Influence of high magnetic fields on the superconducting transition of one-dimensional Nb and MoGe nanowires. *Phys. Rev. Lett.* **94**, 17004 (2005).
29. Zgirski, M. & Arutyunov, K. Yu. Experimental limits of the observation of thermally activated phase-slip mechanism in superconducting nanowires. *Phys. Rev. B* **75** 172509 (2007).
30. Shah, N., Pekker, D. & Goldbart, P. M. Inherent stochasticity of superconductive–resistive switching in nanowires. *Phys. Rev. Lett.* **101**, 207001 (2008).
31. Tinkham, M., Free, J. U., Lau, C. N. & Markovic, N. Hysteretic *I–V* curves of superconducting nanowires. *Phys. Rev. B* **68**, 134515 (2003).
32. Langer, J. S. & Ambegaokar, V. Intrinsic resistive transition in narrow superconducting channels. *Phys. Rev.* **164**, 498–510 (1967).
33. McCumber, D. E. & Halperin, B. I. Time scale of intrinsic resistive fluctuations in thin superconducting wires. *Phys. Rev. B* **1**, 1054–1070 (1970).
34. Tinkham, M. *Introduction to Superconductivity* 2nd edn, Ch. 8 (McGraw-Hill, 1996).
35. Fulton, T. A. & Dunkleberger, L. N. Lifetime of the zero-voltage state in Josephson tunnel junctions. *Phys. Rev. B* **9**, 4760–4768 (1974).
36. Rogachev, A., Bollinger, A. T. & Bezryadin, A. Influence of high magnetic fields on the superconducting transition of one-dimensional Nb and MoGe nanowires. *Phys. Rev. Lett.* **94**, 017004 (2005).
37. Tinkham, M. & Lau, C. N. Quantum limit to phase coherence in thin superconducting wires. *Appl. Phys. Lett.* **80**, 2946–2948 (2002).
38. Bollinger, A. T., Rogachev, A., Remeika, M. & Bezryadin, A. Effect of morphology on the superconductor–insulator transition in one-dimensional nanowires. *Phys. Rev. B* **69**, 180503 (2004).

Acknowledgements

This material is based on work supported by the US Department of Energy, Division of Materials Sciences under Award No. DE-FG02-07ER46453, through the Frederick Seitz Materials Research Laboratory at the University of Illinois at Urbana-Champaign. M.-H.B. acknowledges the support of the Korea Research Foundation Grant No. KRF-2006-352-C00020.

Author contributions

M.S. fabricated all of the nanowire samples; M.S., M.-H.B., A.R. and A.B. carried out all of the measurements; M.S., M.-H.B., D.P., N.S., T.-C.W., P.G. and A.B. worked on the theoretical modelling, data analysis and co-wrote the paper. All authors discussed the results and commented on the manuscript.

Additional information

Supplementary information accompanies this paper on www.nature.com/naturephysics. Reprints and permissions information is available online at http://npg.nature.com/reprintsandpermissions. Correspondence and requests for materials should be addressed to M.S.